

Transverse loading of monofilament reinforced microcomposites: a novel fragmentation technique for measuring the fibre compressive strength

H. D. WAGNER

Department of Materials and Interfaces, The Weizmann Institute of Science, Rehovot 76100, Israel

C. MIGLIARESI

Department of Engineering, The University of Trento, Mesiano 38050, Trento, Italy

A. H. GILBERT, G. MAROM

Casali Institute of Applied Chemistry, Graduate School of Applied Science and Technology, The Hebrew University of Jerusalem, Jerusalem 91904, Israel

Carbon/J-polymer single fibre composite samples were tested under tensile conditions with the fibre direction perpendicular to the tensile loading axis. The Poisson ratio effect induced a compression strain field in the fibre, resulting in a fragmentation phenomenon similar to that observed in a fibre subjected to tensile loading. This observation introduces a novel technique for the measurement of the compressive strength of single fibres, calculated either from the stress at first break, or from the Weibull scale parameter obtained from the fragmentation data produced at various stress levels. The special sample loading configuration used here also provides the first measurement of the effect of the length of the fibre on its compressive strength value.

1. Introduction

Model unidirectional composites, termed microcomposites, made of single fibres accurately positioned and aligned within a thin polymer film, are useful from a variety of view-points. For example, in fracture studies [1] microcomposites may provide direct evidence for damage theories, while single or multi-filament monolayers may be used in detailed studies of the fragmentation phenomenon [2-4].

A recent paper outlines the main conceptual principles of microcomposites, and demonstrates them by a number of experimental observations [5]. On the conceptual level it is claimed that microcomposites are rendered a potentially ideal experimental tool by which theoretical models can be checked. This results from a situation where microcomposites accurately simulate the unidirectional lamina, which is the fundamental structure considered by most theoretical models of composites. A microcomposite is regarded as the test tube of the composite material scientist, by which fundamental scientific factors can be examined. The scaling-up from the microcomposite to the real structure enables a systematic study of possible deviations from the ideal structure of the unidirectional lamina. This is done by adding perturbations to the models in a controlled manner, that selectively probe the effects of various scaling-up geometrical or material parameters.

The experimental examples in Reference 5 focus on the usefulness of microcomposites for checking existing theoretical models in the low fibre content range. The fit in that range is often ignored, even though it is sometimes precisely in that range that sharp variations in behaviour are predicted. Examples are the mechanical strength, for which a minimum is predicted for a very low, non-zero, fibre content [6], and the thermal expansion, for which an abrupt decrease in the coefficient of thermal expansion is predicted by theory [7].

Transverse loading of monofilament reinforced microcomposites was performed in an attempt to study the fibre/matrix interaction in carbon fibre reinforced thermoplastic matrix composites. Originally, the idea was to examine how the thermal history of the composite and the resulting matrix crystallinity and fibre/matrix interfacial transcrystallinity were reflected in the transverse strength. This goal soon became secondary in light of the discovery that under such loading circumstances the carbon filament failed in compression. This compressive failure phenomenon, resulting from the transverse Poisson contraction, continued beyond the stage of first fibre break, until either break saturation or matrix yielding occurred. Below the saturation limit, the loads at first and each successive break could result in the average compressive strength of the filament (at progressively

smaller fibre lengths), while the mean break length at saturation (if reached) could produce the critical length, and in turn, the fibre/matrix interfacial bond strength.

For comparison, a valid experimental procedure reported in the literature for compressive testing of single filaments is based on flexural testing of beams, with a monofilament embedded in the compressive section of the beam [8, 9]. One of very few available examples of the fragmentation method in compression is given [9]. Although the fragmentation method for measuring the average critical length and for calculating the interfacial bond strength is well established, it is practiced almost exclusively in tension [10]. Other methods to determine the axial compressive strength of fibres include the loop test (or elastic method) [11] and indirect, rule-of-mixtures based estimations from compressive testing of unidirectional composites [12].

The purpose of this paper is to report on several preliminary observations, and to outline a number of avenues for further research. Accordingly, two main efforts were conducted as follows: one was aimed at assessing the feasibility of the new method of compressive strength testing of single filaments. Another effort was designated to evaluate the newly observed fragmentation process in compression, and to compare it to the familiar techniques either in tension or in compression. Of particular interest was the newly offered possibility of fibre length (size) effect study in compression, based on measuring the effect of fibre fragment length on the compressive strength, as recently proposed for tensile fragmentation (see below) [2, 4].

2. Experimental procedure

The matrix of the monofilament microcomposites was J-1 polymer, a polyamide homopolymer based on bis(para-amino cyclohexyl) methane (PACM), by Du Pont. A number of J-polymer experimental materials are available, whose microstructures vary according to the composition and the thermal history [13, 14]. In the J-1 polymer, for example, the amorphism – crystallinity balance – as well as the type of crystallinity are determined by the thermal history [15]. Under cooling conditions that enable crystallization, a high cooling rate produces a higher melting point and a kinetically favoured crystallinity, while a slow rate results in a lower melting point, and a thermodynamically preferred structure.

The importance of the thermal history calls for an accurate definition of the microstructure as well as of the mechanical properties for each manufacture procedure employed. In this paper, results of only one manufacture routine are presented. That routine subjected the J-polymer matrix of the monofilament microcomposite to the following thermal cycle, designated quenching, Q . It consisted of melting and pressing the as-received polymer at 320 °C for 20 min, followed by quenching in ice water. Fig. 1 presents the differential scanning calorimetry trace at 20 °C min⁻¹ of the Q matrix. This matrix, which is virtually amorphous, exhibits a glass transition at 140 °C,

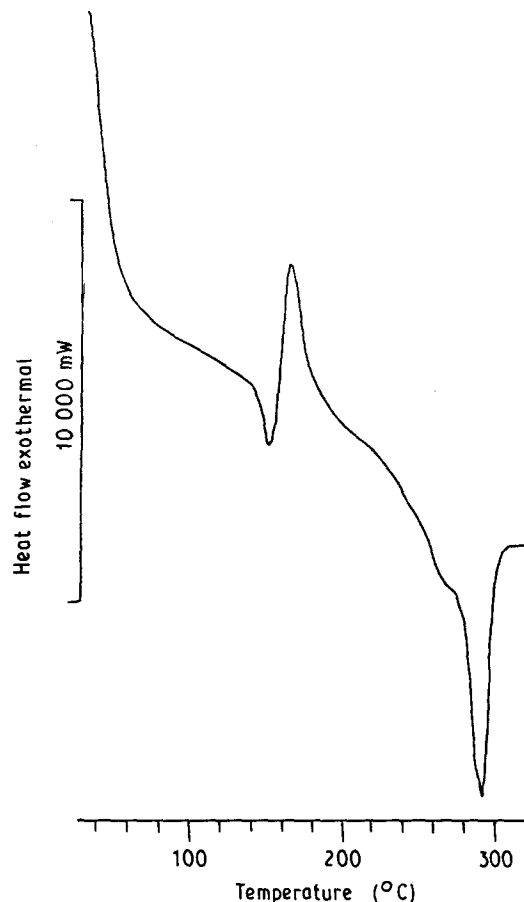


Figure 1 A differential scanning calorimetry trace of quenched J-1 polymer.

followed by recrystallization at 144 °C, by a melting shoulder at 260 °C, and by a major melting peak at 280 °C. This is in agreement with the characteristics of the as-received J-1 polymer, as described [15]. A detailed analysis of the effect of thermal history on the microstructure and the mechanical properties is beyond the scope of this paper, and will be discussed together with results from a wider range of thermal treatments in papers to come.

The carbon fibres employed as monofilament reinforcements were of two types. The first was the low modulus PRD-172 pitch-based fibre (Du Pont), of a nominal tensile strength and modulus of 2.0 and 260 GPa, respectively [16], and the second was ACIF-HT PAN-based fibre (Afikim Carbon Fibers), of a nominal tensile strength and modulus of 2.9 and 230 GPa, respectively. The pitch-based fibre (denoted LM) was an untreated and unsized type, while the PAN-based (denoted HT) was an electrochemically oxidized fibre, with its epoxy emulsion size washed off in acetone prior to sample preparation.

Microcomposite samples approximately 100 µm thick were prepared by carefully placing parallel individual monofilaments at 2 cm intervals, sandwiched between four rectangles (8 cm × 4 cm) of dried, as-received J-polymer. The J-polymer was pressed between two 1 mm thick stainless steel plates of the same dimensions. Kapton polyimide sheet (Du Pont) coated with Freekote 44 and Freekote HMT release agents (Hysol) was placed between the J-polymer and the steel plates to ensure easy release of the samples.

Processing was performed at 320 °C for 20 min using a Carver press with minimal applied pressure, followed by quenching in ice water. Mini-tensile samples 3 mm wide were carefully cut from the prepared sheets under a microscope, ensuring that a single, straight monofilament perpendicular to the sample axis could be observed half way along its length. Cardboard grips (1 cm²) were glued to the ends of the sample using Poxipol room temperature curing epoxy resin, giving a sample gauge length of 20 mm. Post-curing was performed at 60 °C for 1 h under pressure to prevent sample slippage during testing. Samples were loaded, as described schematically in Fig. 2, at a rate of extension of 0.83 μm s⁻¹ using an elaborate video-monitored tensile testing system described in detail elsewhere [1, 2, 4]. The lengths of the fibre fragments at each stress level were measured by means of a Colorado video micrometer (Model 305A), with an estimated accuracy of 5 μm.

2.1. Theoretical background

The calculation of the compressive strength of the fibre is based on the following considerations pertaining to a schematic description of the test configuration in Fig. 2. The fibre failure in compression results from a Poisson contraction effect along the *y* axis, induced by a tensile stress applied in the *x* direction. Considering the sample in Fig. 2, an orthotropic lamina whose natural longitudinal (*L*) and transverse (*T*) directions coincide with the *y* and *x* axes, respectively, the strain in the *L* direction is given by

$$\varepsilon_L = \sigma_L/E_L - \nu_{TL}(\sigma_T/E_T) \quad (1)$$

where σ and ε denote stress and strain and E and ν denote Young's modulus and Poisson's ratio, respectively. Taking $\varepsilon_f = \varepsilon_L$ and $\sigma_L = 0$, where ε_f is the longitudinal strain in the fibre, Equation 1 reduces to

$$\varepsilon_f = -\nu_{TL}(\sigma_T/E_T) \quad (2)$$

Assuming a perfect fibre/matrix interface, $\varepsilon_f = \sigma_f/E_f$, where σ_f and E_f are the compressive stress and modulus of the fibre, taking $\nu_{TL} = \nu_m$ (which is justified for a very low fibre volume fraction ϕ_f , obtained by substituting $\phi_f = 0$ in the expression for ν_{TL} [17]), and taking $E_T = E_m$, where m denotes matrix property, Equation 2 results in

$$\sigma_f = -(\nu_m E_f/E_m) \sigma_T \quad (3)$$

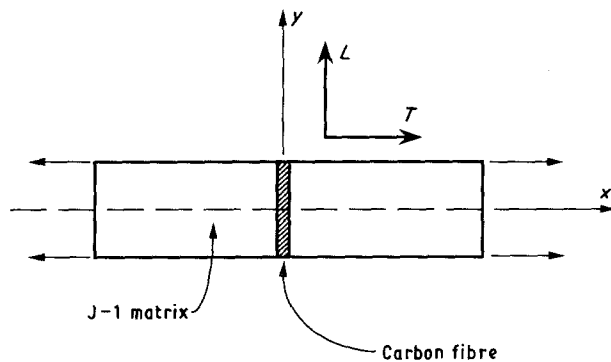


Figure 2 A schematic depiction of the test specimen, showing the loading and the fibre axis directions.

which for each fibre break transforms to

$$\sigma_{fu} = -(\nu_m E_f/E_m) \sigma_{Tu} \quad (4)$$

where the subscript *u* denotes an ultimate value, and σ_{Tu} is the value of the stress applied to the sample when the fibre break occurs.

The fragmentation test, either in tension or in compression, enables a calculation of the fibre critical length, l_c , from the average fragment length at saturation, l_a , by the Kelly–Tyson approach as follows:

$$l_c = (4/3) l_a \quad (5)$$

In turn, the fibre/matrix interfacial shear strength, τ , can be calculated by Equation 6, where d is the fibre diameter

$$\tau = (\sigma_{fu}d)/(2l_c) \quad (6)$$

Here σ_{fu} is the strength of the fibre at l_a .

A recent paper [4] showed that in fact the entire loading history of a single fibre in a fragmentation test can be utilized to measure the size effect on fibre strength. This has the important practical advantage that the fibre strength at the saturation length (needed in Equation 6) is readily obtained from the fragmentation test itself (*in situ* technique), rather than from multiple single fibre testing (*ex situ* technique) as done usually. It was shown [4] that the size effect could be determined by a continuously monitored experiment which yields a set of fragment lengths as a function of the applied stress, according to Equation 7 as derived from the Weibull weakest link model

$$s_a = \alpha^\beta \sigma_{fu}^{-\beta} [\Gamma(1 + 1/\beta)]^\beta \quad (7)$$

where α and β are the Weibull scale and shape parameters for strength, respectively, Γ is the gamma function and s_a is the average fragment length for a stress level σ_{fu} (which becomes l_a at break saturation). The arguments presented in Reference 4 for a tensile loading situation are valid in principle for the compressive loading situation investigated.

3. Results and discussion

The essential features of a fragmentation experiment with the HT PAN-based fibre loaded perpendicular to the fibre axis direction are shown in Fig. 3, as observed through an optical microscope. Fig. 3a illustrates a higher magnification photograph of a single break, showing the diagonal fracture path typical of compressive failure, while Fig. 3b exemplifies a stage in the propagation of the fragmentation process, showing a number of fragments of different lengths.

Table I presents the results of the compressive strength determined at first break for the two fibre types, as calculated by Equation 4 where $\sigma_{fu} = \sigma_f^{\text{comp}}$. The properties of the matrix in the *Q* state $\nu_m = 0.345$ and $E_m = 2.2$ GPa were taken from [14], and it was assumed that the compressive Young's moduli of the fibres were equal to the tensile values. The σ_{fu} values are averages of 3 and 7 tests (with around 8% deviations) for the HT and LM fibre, respectively. Table I also lists the stress recorded at first break, σ_{Tu} , and the ratio of the compressive to the tensile strength.

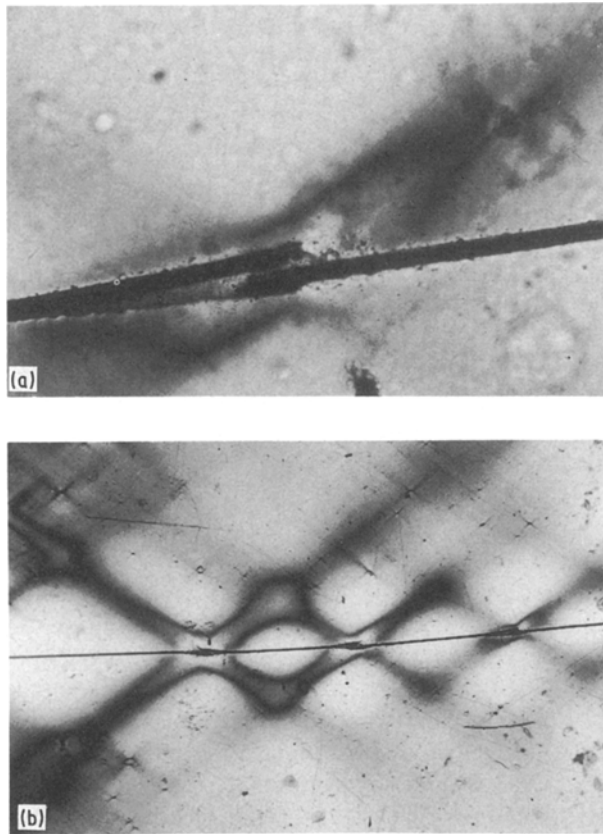


Figure 3 (a) A typical single break and (b) sequence of breaks formed in a fragmentation experiment of an HT PAN-based carbon fibre as observed by polarized light microscopy.

TABLE I The compressive strengths and the compressive-to-tensile stress ratios of two carbon fibres

Fibre	E_f (GPa)	σ_{Tu} (MPa)	σ_f^{comp} (MPa)	$\sigma_f^{comp} / \sigma_f^{tens}$ (%)
HT	230	24.6	888	29.7
LM	260	32.2	1313	66.4

Clearly, Equation 4 used for the calculation of the compressive strength, does not account for residual thermal stresses which, depending on the thermal treatment history, may stem from the difference in thermal expansion between fibre and matrix. The residual thermal stress effect, neglected here, could be estimated and accounted for [9].

The compressive strength of the PAN-based carbon fibre (HT) is lower than that of the pitch-based (LM), and for both fibres the compressive strength is about half the tensile strength. For comparison, Ohsawa *et al.* [9] report a compressive strength (and its proportion) of 2.06 GPa (58.9%) for a PAN-based T-300 fibre and of 1.25 GPa (37.4%) for a low modulus pitch-based fibre. It has been pointed out by other researchers that the compressive strength depends on the fibre type, i.e. carbon versus graphite, with higher strengths in the lower modulus carbon fibre. Also, the fibre origin plays a role, with the PAN-based fibre usually exhibiting higher strengths compared with the pitch-based. Reported compressive strengths for various PAN-based fibre are 2–4 times higher than our

results, while those for the pitch-based fibres are in very good agreement [18, 19].

The fragmentation procedure to measure the size effect on the compressive strength of the fibre was performed by analogy to the procedure proposed for tensile loading [4]. The analysis was carried out according to Equation 7, where the compressive strength of the fibre, σ_{fu} , is given as a function of the transverse tensile stress by Equation 4. Using Equation 7 a plot of $\ln s_a$ against $\ln \sigma_{fu}$ yields a straight line with a negative slope equal to the Weibull shape parameter, β . The Weibull scale parameter, α , can then be calculated from the value of the intercept, which is equal to $\beta \{ \ln \alpha + \ln [\Gamma(1 + 1/\beta)] \}$.

Fig. 4 shows representative results for both the LM and HT fibres, where the fragment length (measured with a video micrometer) is plotted against the fibre stress in logarithmic co-ordinates. Note that this is the first time that actual fragment length data have been presented. In previous publications by one of these authors (HDW), the average length data were used, obtained by dividing the initial sample length by the number of fragments at a given stress level. Experimental data were generated mostly with LM fibres and, for comparison, one HT fibre sample was studied. As predicted by the Weibull model (Equation 7), the data fit a straight line reasonably well for both fibre types (Fig. 4). Moreover the saturation limit does not seem to be reached as no deviation from linearity is apparent at the latest stages of the fragmentation tests. This is unlike the situation in a tensile fragmentation test, and may be attributed to the occurrence of matrix yielding and/or fibre–matrix interface debonding (Fig. 3a) at stresses below the saturation limit.

The Weibull shape and scale parameters obtained from the transverse fragmentation tests are listed in Table II. The scale parameter reflects the mean compressive strength at unit length, and as seen from Table II, the values for both fibre types are in good agreement with those derived from the first break data listed in Table I. Some comments are necessary concerning the results for the shape parameter, which show a large sample-to-sample variability. The data for the first two samples, J34 and J40, show a relatively poor fit to a straight line as seen from the value of the correlation coefficient, r^2 . Thus, if only the data of samples J41, J44, and J45 are considered, the shape parameter varies between 8.4 and 14.9. This is about 2–3 times the value of the shape parameter usually obtained from data based on a single length for the same fibre, which for carbon fibres is about 4–7 (in tension, however). Interestingly, the same difference, as well as high variability is observed for the scale parameters as obtained from tension data at a single length and from the slope of $\ln(\text{strength})$ against $\ln(\text{length})$ data using other fibres such as Kevlar [20]. Thus apparently the same discrepancy (and variability) between the shape parameter values obtained from independent experimental measurements under tensile testing conditions is observed under compressive conditions although strictly speaking no compression data here were obtained at a single fibre length.

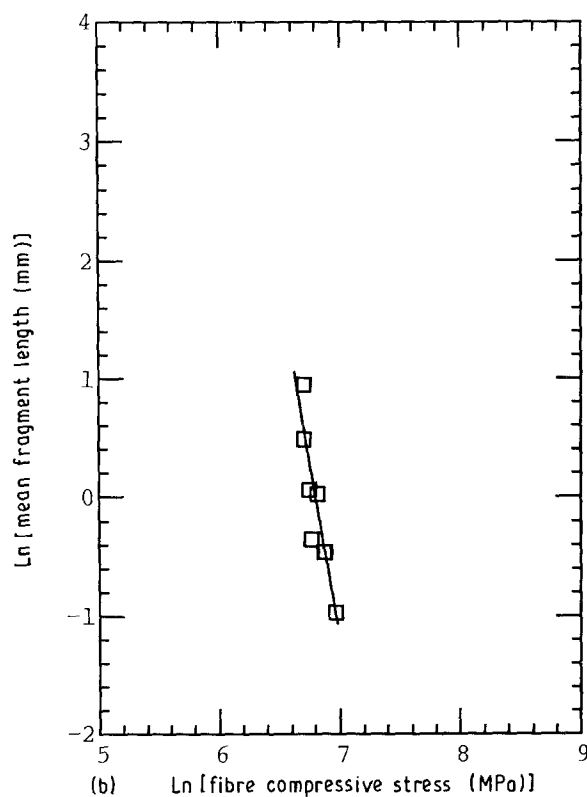
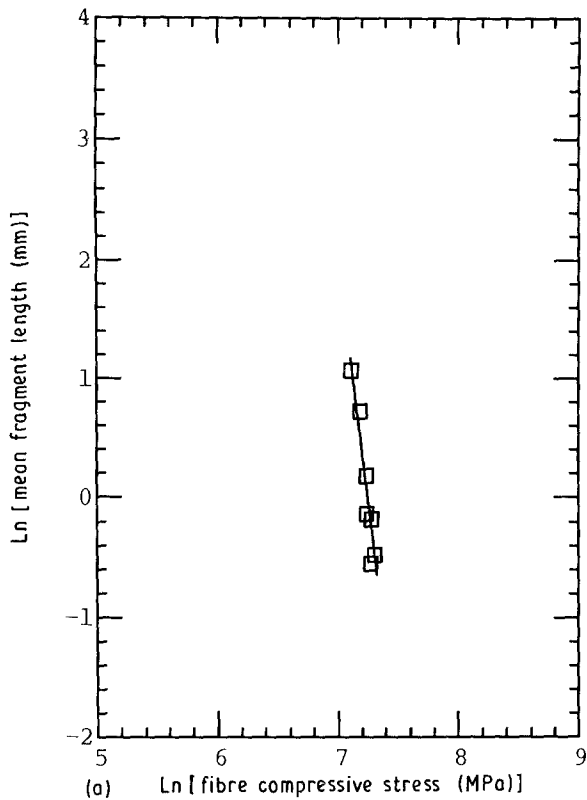


Figure 4 Representative plots for both: (a) LM and (b) HT fibres, where the fragment length is plotted against the fibre stress in logarithmic coordinates.

It should be noted that saturation is very difficult to achieve under such loading, due to prior yielding in the polymer matrix, and that fragmentation phenomena appear to be intrinsically more difficult to achieve in compression than in tension. In addition, it should be clearly understood that factors such as the ultimate compressive failure strain of the fibre, and the degree of interfacial debonding that occurs will ulti-

TABLE II Weibull shape and scale parameters for both fibre types. Also presented are values for the correlation coefficient r^2 derived from the linear regression lines in the ln-ln plots similar to Fig. 4

Sample	Weibull parameters		Correlation coefficient, r^2
	Shape, β	Scale, α (MPa)	
LM			
J34	4.8	1449.9	0.21
J40	30.5	1510.0	0.41
J41	12.5	1470.4	0.94
J44	14.9	1547.7	0.83
J45	8.4	1492.5	0.88
HT			
J85	6.0	967.1	0.80

mately determine the viability of this kind of experiment.

4. Conclusions

Transverse loading of monofilament reinforced microcomposites is proven to be useful for the determination of the compressive properties of the fibre. The calculation of the compressive strength of the fibre is straightforward, and is based directly on the level at first break of the applied stress. A study of the fibre length (size) effect under *in situ* conditions is also possible, based on a Weibull weakest link analysis of the fragmentation process. It is feasible that in a fragmentation experiment that achieves break saturation, the fibre critical length may also be calculated. This, however requires a careful selection of a matrix that does not yield prematurely, and which gives sufficient bonding to the fibre.

Acknowledgement

H. D. Wagner is the Incumbent of the J. and A. Laniado Career Development Chair.

References

1. H. D. WAGNER and L. W. STEENBAKKERS, *J. Mater. Sci.* **24** (1989) 3956.
2. H. D. WAGNER and A. EITAN, *Appl. Phys. Lett.* **56** (1990) 1965.
3. A. EITAN and H. D. WAGNER, *ibid.* **58** (1991) 1033.
4. B. YAVIN, H. E. GALLIS, J. SCHERF, A. EITAN and H. D. WAGNER, *Polym. Compos.* **12** (1991) 436.
5. H. D. WAGNER, M. RUBINS and G. MAROM, *Polym. Compos.* **12** (1991) 233.
6. M. R. PIGGOTT, in "Load Bearing Fibre Composites" (Pergamon Press, Oxford, 1980) p. 101.
7. R. A. SCHAPERLY, *J. Compos. Mater.* **2** (1968) 380.
8. S. J. DETERESA, S. R. ALLEN, R. J. FARRIS and R. S. PORTER, *J. Mater. Sci.* **19** (1984) 57.
9. T. OHSAWA, M. MIWA, M. KAWADE and E. TSUSHIMA, *J. Appl. Polym. Sci.* **39** (1990) 1733.
10. W. D. BASCOM, R. M. JENSEN and L. W. CORDNER, in Proceedings of ICCM VI and ECCM 2 (Elsevier Applied Science, UK, 1987).
11. W. R. JONES and J. W. JOHNSON, *Carbon* **9** (1971) 645.
12. J. H. SINCLAIR and C. C. CHAMIS, *ASTM STP* **808** (1983) 155.
13. I. Y. CHANG and J. K. LEES, *J. Thermoplast. Compos. Mater.* **1** (1988) 277.

14. A. R. WEDGEWOOD, K. B. SU and J. A. NAIRN, *SAMPE J.* **24** (1988) 41.
15. W. J. LEE, B. K. FUKAI, J. C. SEFERIS and I. Y. CHANG, *Composites* **19** (1988) 473.
16. H. D. WAGNER, J. ARONHIME and G. MAROM, *Proc. Roy. Soc. London A*, **A428** (1990) 493.
17. R. L. FOYE, *J. Comp. Mater.* **6** (1972) 293.
18. H. M. HAWTHORNE and E. TEGHTSOONIAN, *J. Mater. Sci.* **10** (1975) 41.
19. A. KITANO, T. NORITA and K. NOGUCHI, in Proceedings of the 12th Fukugo Zairyo Symposium Kohen-Yoshishu, (1987) p. 125.
20. H. D. WAGNER, S. L. PHOENIX and P. J. SCHWARTZ, *J. Compos. Mater.* **18** (1984) 312.

*Received 5 April
and accepted 30 July 1991*